A Sensitivity Analysis of DAS Lifetime Collision Probability Estimates

Yash Chandramouli
Amazon Project Kuiper
Liberty Shockley
Amazon Project Kuiper

ABSTRACT

As space safety becomes paramount in spacecraft design, there is a growing need for precision and transparency in the available tools for analyzing the on-orbit and reentry risk of a given space mission. Programs like NASA's Debris Assessment Software (DAS) or ESA's Debris Risk Assessment and Mitigation Analysis (DRAMA) tool are commonly used to calculate critical space safety metrics such as satellite deorbit time, lifetime collision probability, and reentry human casualty risk as a part of the initial regulatory licensing process. However, these models are designed primarily as compliance assessment tools, with limited options to assess multiple spacecraft configurations simultaneously and with little visibility into internal computations. These factors make it prohibitively labor-intensive for spacecraft designers to explore large trade spaces or derive useful insights when considering mission space safety impacts during initial trade studies. Additionally, without insight into what design changes might affect the final computations, the space safety impact of a system is often only assessed at the time of licensing, not accounting for the impacts of mission and satellite architecture changes that might occur throughout the design lifetime of the spacecraft. With no analytical method of computing these metrics, a spacecraft mission designer who wishes to incorporate space safety metrics into their system trade space is forced to iteratively "guess-and-check" to design mission trajectories that comply with regulatory requirements.

Sensitivity studies on input parameters could provide a window into these complex models and give spacecraft mission designers the tools they need to continually and efficiently assess their compliance with space safety regulations throughout the satellite design process. Sensitivity analysis methods aim to capture the impact that input parameter variations have on the output of a model. These methods can be local or global. Local methods, such as one-at-a-time (OAT) methods, capture the sensitivities around a baseline input set, often by modifying a single variable at a time and tracking the corresponding changes in the output. Global methods instead aim to capture a broader picture of sensitivities across a wide range of datapoints. One global method is estimating the partial derivatives of a surrogate model mapping the output with respect to the input, often by extracting the coefficients from a regression model. Another commonly used global method is Sobol's method that computes "sensitivity indices" which represent the proportion of the output variance that is captured by knowledge of a subset of input variables. While analytically difficult to solve for, these indices can be estimated to high accuracy through Monte Carlo analyses.

This paper presents an approach that uses global sensitivity analysis to help spacecraft mission designers more efficiently prioritize and explore the trade space around a given space safety metric. Specifically, this paper focuses on assessing the sensitivity of DAS outputs of lifetime large object collision probability. After generating a dataset of space mission profiles across LEO, we then compute Sobol indices with respect to inputs such as satellite semi-major axis, inclination, deorbit year, and area-to-mass ratio. We then discuss novel insights showed by this analysis. Lastly, we demonstrate how sensitivity analysis can be used by spacecraft mission designers to prioritize changes to their system, estimate the impact of variations in parameters, and compute equivalent changes to then be passed into broader system-level trade studies.

The final results report new DAS performance data that are valuable to spacecraft operators and regulators, and provide valuable insights and tools to spacecraft designers who wish to incorporate space safety concerns into their trade studies. The method presented can also be extended to other space safety model outputs such as satellite reentry casualty risk or small object collision probability.

1. BACKGROUND

The ongoing emergence of commercial space ventures necessitates well-understood tools for the evaluation of space safety risk. Two such industry-standard tools that are commonly used for this purpose are the National Air and Space Administration's (NASA) Debris Assessment Software (DAS) and the European Space Agency's (ESA) Debris Risk Assessment and Mitigation Analysis (DRAMA). These tools are often used to assess whether a given space mission is compliant with space safety regulations. In particular, DAS is often used by operators in Federal Communications Commission (FCC) filings to verify compliance with regulated space safety metrics such as satellite passive deorbit time, small object collision probability, large object collision probability, and reentry casualty risk. By inputting satellite mission and design parameters such as mission year, orbital elements, and mass, an operator can easily determine whether their mission meets regulatory thresholds for these metrics. While the methods within this paper can and should be applied to other models, this paper chooses to focus on NASA's DAS because of its preeminence within the United States.

Spacecraft designers also regularly use DAS during the spacecraft design process, rather than just as a part of the filing process. For example, DAS reentry casualty risk estimates are often used to ensure that satellite components demise during atmospheric reentry [9]. This is a valuable use case that expands the capabilities of tools like DAS by enabling operators to continuously monitor space safety performance, evaluate space safety parameters as part of the larger design trade space, and assess the impacts of improvements or changes to their system between the time of filing and the time of launch. However, since DAS is not designed explicitly for this purpose, its effectiveness as a design tool is artificially limited. DAS analyses require manual user inputs and can only process a single scenario at a time which hinders the exploration of a large-scale trade space. Some outputs, such as reentry survivability and small object collision probability, require the user to input geometric and material data in tree structures that are manually intensive to populate and not easy to modify. Lastly, it is not currently possible to adjust the various assumptions in the software regarding solar weather, atmospheric drag, orbital debris distribution, and reentry trajectories. The basic space environment assumptions are outlined in the user manual, but the user must consider DAS a black box on how they are implemented and any other assumptions made. These limitations mean that while DAS has the potential to serve as a valuable tool to aid users in incorporating space safety metrics into the satellite design process, it is still currently best used as a quick and effective compliance assessment tool.

This study demonstrates how sensitivity analysis methods can help bridge this gap between the designed purpose of DAS and its potential use cases by providing a deeper understanding of how DAS outputs are affected by changes in their input spacecraft and mission parameters. Similar work was previously done for deorbit lifetime which is a metric with well-understood physical relationships between inputs and outputs [6]. This paper extends those same methods to DAS estimates of large object collision probability, though the same methodology can and should be applied to other models and metrics as well. The resulting insights provide a window into input/output relationships that were previously within a "black box", provide tools for design engineers to quantitatively and qualitatively include lifetime collision risk in their design and trade studies, and highlight the importance of accounting for model sensitivities when assessing a space mission's space safety metrics at the time of launch.

This paper is a description of a method for analyzing predictive risk assessment models using DAS as an example, rather than a comment on current regulations or representations made in specific licensing proceedings.

1.1 NASA's Debris Assessment Software (DAS)

The NASA Debris Assessment (DAS) software was first developed in 2007 to aid NASA programs in assessing compliance with NASA Technical Standard 8719.14, *Process for Limiting Orbital Debris* [14]. It drives how the DAS software is designed and is applied to all NASA Missions, and to other space missions seeking a radio frequency license from the Federal Communications Commission (FCC).

For part 5 experimental applications, used for non-revenue generating and new technology spacecraft, 47 CFR §5.64(b) of the [Federal Communication] Commission's rules applies. Specifically, excerpts from §5.64(b)(4)(i) require:

> (A) A demonstration that the space station operator has assessed and limited the probability of collision between any space station of the system and other large objects (10 cm or larger in diameter) during the total orbital lifetime of the space station, including any de-orbit phases, to less than 0.001 (1 in 1,000)....The collision risk may be assumed zero for a space station during any period in which the space station will

be maneuvered effectively to avoid colliding with large objects.

In the United States, DAS is often used to assess space safety compliance at the radio frequency licensing phase, which can be months or years prior to the launch of a built satellite. During that intervening period, mission needs and anomalies can change the orbital and physical parameters of the spacecraft, causing the real-life scenario to stray from the approved configuration. Having a way to incorporate these compliance assessment tools into the trade space can enable mission designers to utilize them past the point of radio frequency licensing to ensure that their satellites remain compliant up until launch. DAS orbital element inputs are done in the form of classical Keplerian elements, abbreviated in Table 1.

Table 1: Orbital Elements in DAS

Symbol	Orbital Element	Unit
a	Semi-major axis	km
e	Eccentricity	-
i	Inclination	degrees
Ω	Right ascension of the ascending node (RAAN)	degrees
ω	Argument of perigee	degrees
M	Mean anomaly	degrees

Apogee, r_a, the point farthest from the Earth in its orbit, and perigee, r_p, the closest point to the earth in orbit, can be found directly from the semi-major axis and eccentricity:

$$r_a = a(1+e) \tag{1}$$

$$r_p = a(1-e) \tag{2}$$

DAS can evaluate payloads operating from 2016 to 2130 (114 years), and non-operating payloads (collectively, space objects), until 2270 (254 years) [14]. These constraints come from the Orbital Debris Engineering Model (ORDEM), which models solar flux based on year for current and predicted debris fields, and which is used by DAS to compute cumulative orbital collision probability [19].

ORDEM computes collision probabilities by estimating fluxes of debris for a given year. In LEO these fluxes are modeled for objects greater than 10 micrometers, however for this study the large object collision probability only looks at the fluxes for objects larger than 10 centimeters. ORDEM uses in-situ and ground-based radar and optical measurements to scale reference models based on a historical database of known launches, breakups, and maneuvers. This study was done using ORDEM 3.2 which uses measurements of the debris population up to 2022 and forward propagates the population in LEO by presuming a repeat of the previous 8-year launch cycle assuming a 90% post-mission disposal success rate [19].

1.2 Factors Impacting Collision Probability

A key factor that impacts satellite lifetime collision probability is the duration of passive deorbit. Passive deorbit lifetime is affected most greatly by atmospheric drag. A simplistic model for the drag force is:

$$F_{drag} = \frac{1}{2}\rho A C_d v^2 \tag{3}$$

Where ρ is the atmospheric density, A is the "wet" area facing the direction of flight, C_d is a dimensionless coefficient of drag, and v is the relative velocity of the satellite with respect to the atmosphere. From this relationship it is clear that the satellite's area to mass ratio ($\frac{A}{M}$) will impact deorbit time and therefore cumulative collision probability - a large surface area space object with minimal weight will be more subject to atmospheric drag than a dense space object with a compact size. Another variable of importance is the atmospheric density (ρ). Numerous models exist for this density, and much active research is dedicated to computing it to higher fidelity. However, the two key general trends

of note for ρ are that it decreases exponentially as altitude increases and that it is impacted by the solar year with density increasing during periods of high solar activity.

Another factor that impacts satellite lifetime collision probability is the distribution of debris on-orbit. Data from ESA's 2024 Space Environment Report [12] captures one estimate of this variability, as seen in Fig. 1. As is visible, the inclinations and altitude that a spacecraft encounters while non-maneuverable greatly impact the amount of debris encountered by the spacecraft and also likely its total lifetime collision probability.

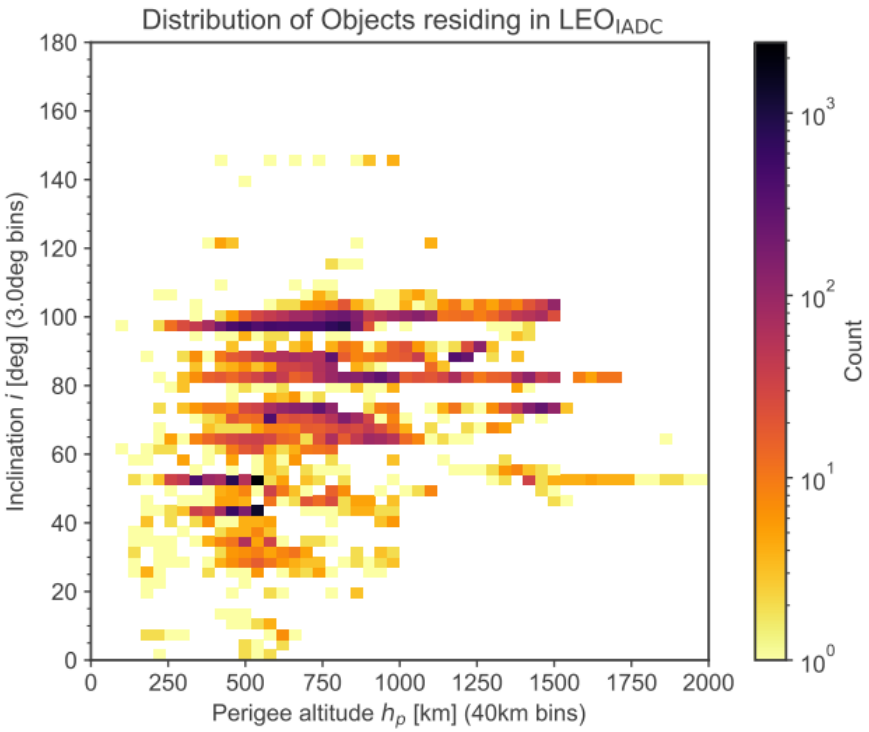

Fig. 1: Count of Objects by Inclination and Perigee Altitude

1.3 Sensitivity Analysis

Sensitivity analysis refers to the field of study concerned with how to allocate the uncertainty of a model output to the uncertainty of its inputs. A model such as DAS has a number of sources of uncertainty including atmospheric model uncertainty and propagation error. However, this paper is concerned with input parameter uncertainty, which is the broad-reaching term to describe any sources of variation that cause the actual parameters input into DAS to differ from the real world parameters. This is common in the context of satellite licensing. Deorbit times are computed optimistically at the time of licensing, oftentimes before an operator has finalized all aspects of their design for production. This means that between licensing and launch, satellite parameters could change and in turn affect potential compliance with space safety standards. Sensitivity analysis allows a satellite designer to account for these downstream effects by understanding the relative impact of changes to input variables on a corresponding output.

Sensitivity analysis methods in the literature can be broadly divided into two groups: local and global methods.

Local Methods Local sensitivity analysis (LSA) refers to methods that capture input sensitivity around a particular data point. A simple approach to this is known as "One-at-a-time" analysis or OAT which looks at the variation of a single input parameter around some baseline point while holding all other input parameters constant. OAT methods have been used in a variety of fields to evaluate the sensitivities of complex models for atmospheric gas transport [4], global climate [11], and long term debris evolution [8]. This method is simple but does not cover the entire state space of solutions, and does not account for the probability density function (PDF) associated with each input parameter.

This in turn means that it fails on nonlinear models with interaction between input variables and on models with large dimensionality. Another LSA method commonly employed is adjoint modeling [3] or another differentiation method to compute the partial derivative of the output with respect to each input. These methods are potentially faster computationally, but still fail to cover the full state space, and are difficult to use on opaque models.

Global Methods Global sensitivity analysis (GSA) refers to methods that evaluate the effect of input parameter variations across the entire state space, oftentimes by looking at large datasets collected via Monte Carlo samplings. A simple GSA method is regression analysis, whereby a linear model is fit to a set of inputs and outputs and the regression coefficients are used as measures of sensitivity. This is simple with low computational cost, but fails to be useful in the case of strongly linear models. Another set of approaches are what are known as screening-based methods. These methods identify which input parameters have the least impact on output variance when fixed, which in turn allows for the ranking of input variables in few model evaluations [5, 10]. These methods are commonly used for their simplicity, but decrease in accuracy when the number of important input parameters is high or unknown. They also only output a ranking of the variables without easily interpretable quantitative outputs, making them of limited value in the spacecraft design use case.

Variance-based methods for GSA are the most suitable for complex black-box models, but at the trade-off of high computational cost. These methods, most commonly Sobol's method [18] and FAST [16], decompose the output variance into the contribution from combinations of each input parameter. Sobol's method does so using Monte Carlo integration loops to yield a set of sensitivity indices that quantitatively represent the relative importance of each input parameter. This method has seen numerous improvements [2, 15, 1] that aim to improve computational speed and extend the method to apply to smaller datasets. FAST (Fourier Amplitude Sensitivity Test) is another variance-based method that represents a function as a Fourier series to decrease computational cost. However, unlike Sobol's method, FAST can only provide first-order effects in a computationally efficient manner.

This paper uses the Sobol method to capture sensitivities. The Sobol method was chosen due to its ability to compute the entire set of sensitivity indices, which is helpful in providing insight into the all aspects of the model across the state space. The Sobol method has also previously been used to compute the sensitivities associated with a model of deorbit lifetime[6], and also combined many of the input parameters to DAS into a single drag correction factor [7].

2. METHODOLOGY

2.1 DAS Standard Cases

This study evaluates a range of standard mission types in LEO for orbital lifetime using the Science and Engineering Utilities in DAS. The ranges chosen for the sensitivity analysis are shown in Table 2.

Table 2: Test Case Bounds

Start Year	Semi-major Axis (km)	Inclination (deg)	Area to Mass (m^2/kg)
2025	6571	0	0.01
2036	6971	90	0.1

The test cases in Table 2 represent a sub-range of the available input ranges in the DAS software. Figure 2 shows where the test cases fall in relation to the percent range of DAS.

While Figure 2 reflects the small range of test cases that could be supported by DAS, the overwhelming majority of satellites launched since 2020 have an Area to Mass ratio ($\frac{A}{M}$) of 0.01 to 0.04 and are in LEO between 300 to 600 km [13]. The chart shows the visual percentage of the dataset vs the range available in DAS, and the colored labels describe the associated mission types assessed in this study. Namely, this study looks at LEO satellites in near-circular prograde orbits, with $\frac{A}{M}$ associated with standard propulsive satellites, and computes their worst-case lifetime collision risk presuming a failure at the operational altitude in the near-term (within the next 11 years).

2.2 Generating Data

Prior to any form of sensitivity analysis, a data set was generated by running the DAS model a number of times that will be referred to as the variable X. This data is generated in line with the modified Sobol method proposed by Saltelli

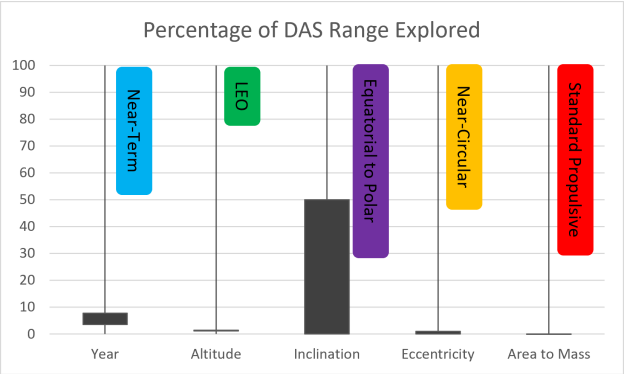

Fig. 2: Data used in sensitivity analysis compared to the functional ranges in DAS

et al [17]. This modified method relies on a procedure for data generation that, if followed, allows the computation of the entire set of Sobol sensitivity indices with just $2d+2$ batches of N data points each, where d is the number of dimensions of the input data set. Therefore:

$$X = N * (2d+2) \tag{4}$$

Due to the long runtime of each DAS run (roughly 1-10 minutes per run), it is in the interest of scalability to decrease X as much as possible. One way to decrease X is through dimensionality reduction of the input. In the case of computing large object collision probability, there are a total of eight potentially relevant input variables: year of passive decay start, perigee altitude, apogee altitude, Ω, i, ω, the average area to mass ratio, and the year of propagation termination. Ω will greatly vary during the course of deorbit due to orbital perturbations, and so it is unlikely that the initial value will matter. Similarly ω can be excluded since the assumption is that the chosen orbits are near-circular. Both variables are therefore fixed at 0 degrees in this study. The propagation end time can be excluded by fixing it at 100 years in the future since for the altitude range of interest (300 - 600 km) deorbit times fall within a reasonable time frame for convergence (i.e., 100 years) in all but the most extreme of cases. Lastly, we assume an eccentricity of near 0 to make initial perigee and apogee roughly equivalent to semi-major axis, which is sufficient to capture a high-level understanding of how starting altitude effects collision probability. This leaves four final input variables - deorbit start year, semi-major axis, inclination, and $\frac{A}{M}$ ratio - for a total of $X = 10N$ runs.

Ten batches of N points were then generated following Saltelli's procedure, with $N = 1024$. This value allows for convergence to within less than 1E-3 in absolute error, as seen in Fig. 3 and Fig. 4. This is sufficient for qualitative comparisons of these indices. First, two $N \times d$ matrices are generated, called A and B, with pseudo-random points uniformly distributed in the interval $[0,1]$. Using these two matrices, a new matrix can be formed by replacing the first column of A with the first column of B, while keeping all other columns the same. Doing this d times (once for each column) yields a total of d matrices of N data points each. These matrices are referred to as $AB_0, AB_1, ...AB_d$ where, for example, AB_0 refers to the matrix formed by replacing the first column of A (zero-indexed) with the first column of B. The same process outlined above can be repeated for matrix B, replacing one column of B with a corresponding column of A and keeping the rest of the columns the same. This yields another d matrices $BA_0, BA_1, ..., BA_d$. Combining these matrices with the original A and B matrices yields a total of $2d+2 = 10$ matrices of N data points each.

Following the input matrix generation, each input data point is mapped to a reference point in the DAS Standard Case interval by shifting and scaling each variable using the following transform:

$$x_{actual} = x_{unit} * (x_{max} - x_{min}) + x_{min} \tag{5}$$

where x_{unit} is the initial value of the variable in the interval $[0,1]$, x_{min} and x_{max} are the minimum and maximum values for the variable respectively as defined in Table 2 above, and x_{actual} is the value of x in the interval $[x_{min}, x_{max}]$.

The final collision probabilities are compiled by running the $10N$ transformed input datapoints through the lifetime collision probability computation in DAS. Traditionally, DAS is only usable in the form of a GUI that is capable of computing a single case at a time, which can make it time-consuming to run large datasets. This paper takes advantage of a Beta version of DAS 3.2.7 that includes Python wrappers of key DAS functions. This enables much faster batch runs with no need for manual input in between runs.

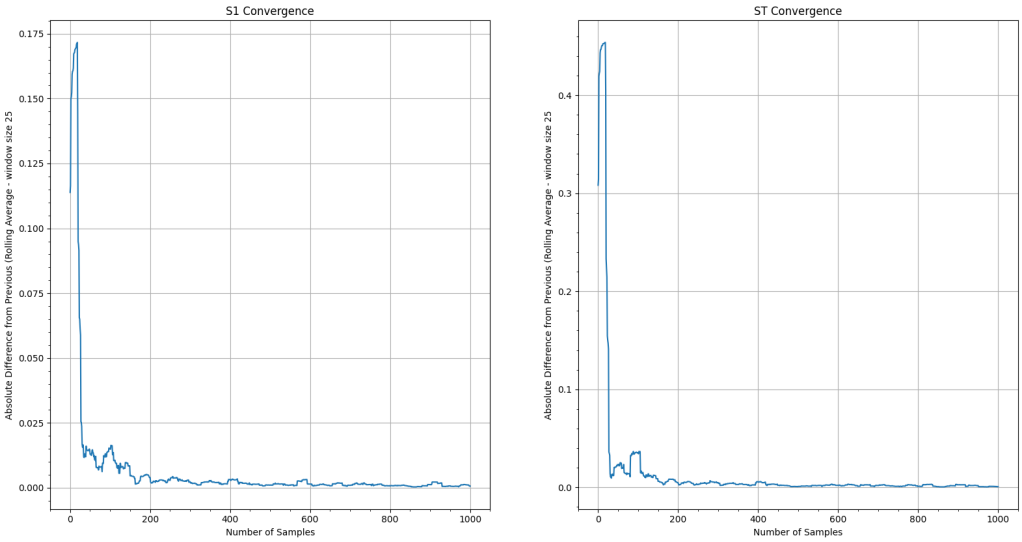

Fig. 3: S1 and ST Convergence Plots

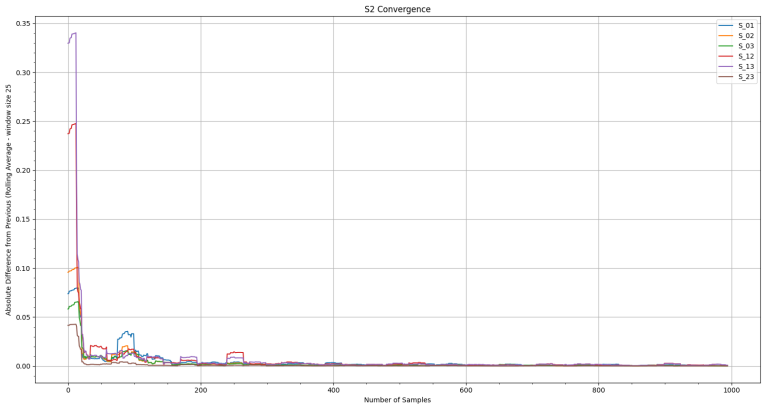

Fig. 4: S2 Convergence Plots

Lastly, in order to view how the sensitivity indices might change as a function of altitude, we conducted the same data generation and index computation for six "semi-major axis bins" spanning 50 km each from 6671 to 6971 km (equivalently 300 km to 600 km altitude). For these cases, we use a value of $N = 500$ for faster computation.

2.3 Computing Sensitivities

The method used to measure the global sensitivity of an output with respect to various input variables is Sobol's Sensitivity Indices [17]. These indices define the proportion of the output variance that can be attributed to a given set of input variables. For a single input variable x_i we refer to what is known as the first-order sensitivity index, defined as:

$$S_i = \frac{Var(E(y|x_i))}{Var(y)} \tag{6}$$

In other words, it answers how much does the given value of x_i affect the spread of y. For example, a variable with little impact would yield little to no change on the distribution of y. Similarly, one can define higher order indices that

correspond to sets of variables. For example, for the variables i and j we can determine that:

$$S_{ij} + S_i + S_j = \frac{Var(E(y|x_i, x_j))}{Var(y)} \tag{7}$$

In essence, S_{ij} captures the additional information on the output when both x_i and x_j are known, rather than when x_i and x_j are independently known. A high value of S_{ij} might indicate that the output is sensitive to an implicit parameter or function of x_i and x_j rather than being directly sensitive to changes in x_i or x_j on their own.

These indices represent the proportional contribution of each set of variables, such that:

$$\sum_{i=0}^{d-1} S_i + \sum_{i<j}^{d-1} S_{ij} + ... + S_{0,1,...d-1} = 1 \tag{8}$$

Finally, a total effect index for each individual variable is determined. These are the sums of all corresponding sensitivity indices for a given variable. For example, in a model with 3 input variables $\{x_0, x_1, x_2\}$ becomes:

$$S_0^T = S_0 + S_{01} + S_{02} + S_{012} \tag{9}$$

and noting that higher-order indices are shared between input variables:

$$\sum_{i=0}^{d-1} S_i^T \geq 1 \tag{10}$$

To directly solve for these variances is not computationally tractable. Therefore, Saltelli et al. [17] demonstrated a method of using Monte Carlo estimators to approximate the indices. These estimators are the drivers behind the data collection method described in Section 2.2. The estimators are presented below, where Y refers to the data points in $\{A, B\}$ and $f(Z)$ refers to the $N \times 1$ matrix of output lifetimes computed by running the collision probability computation in DAS on the data points in matrix Z.

$$S_i \approx \frac{Mean(f(B) * (f(AB_i) - f(A)))}{Var(Y)} \tag{11}$$

$$S_{ij} \approx \frac{Mean((f(BA_i) * f(AB_j)) - (f(A) * f(B)))}{Var(Y)} - S_i - S_j \tag{12}$$

$$S_j^T \approx \frac{1}{2} \frac{Mean((f(A) - f(AB_j))^2)}{Var(Y)} \tag{13}$$

3. RESULTS

3.1 Global Sensitivities

Global sensitivity results for the collision probability computations are presented in Table 4. Sensitivities are denoted by subscripts corresponding to the variable scheme presented in Table 3. Note that in the corresponding Figures, variables are referred to by their numbers (0-3). Non-total sensitivities are listed as percentages since they represent a percentage of the contribution to the total variance. For ease of discussion, semi-major axis results will be reported as pseudo-altitudes (h) relative to the mean Earth radius due to the near circular nature of the orbits considered.

$$h = a - 6371km \tag{14}$$

This altitude will change over an orbit due to orbital eccentricity, but by reporting it as such we can better align these results with the way altitude is discussed in regulatory and general mission design contexts.

Table 3: Variable Mapping

Variable	Variable Number	Mapping
x_y	0	Passive Decay Start Year
x_a	1	Semi-Major Axis
x_i	2	Inclination
x_m	3	$\frac{A}{M}$ Ratio

Table 4: Global First Order and Total Sensitivities

Variable	$S_j(\%)$	S_j^T
x_y	9.812%	0.3636
x_a	51.70%	0.8352
x_i	1.652%	0.0822
x_m	1.526%	0.1175

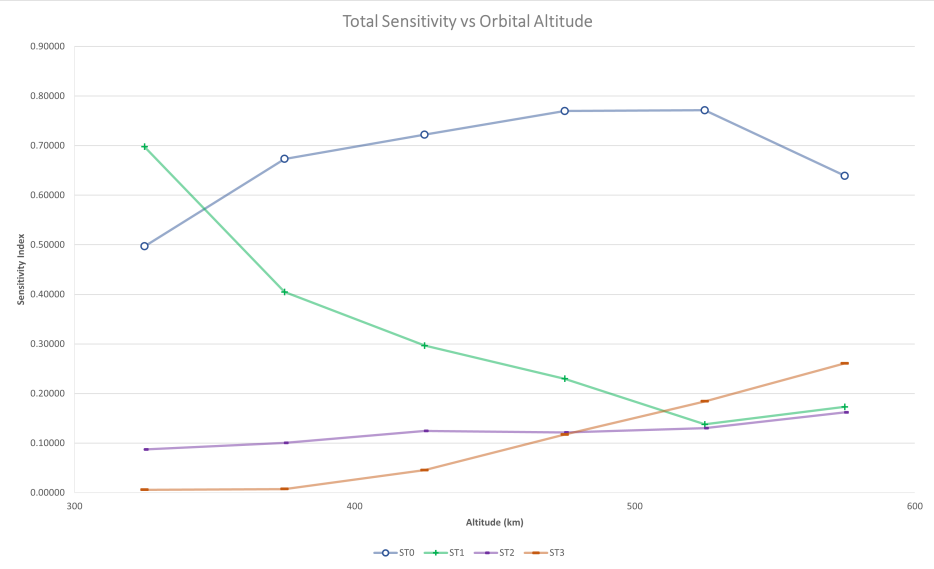

Fig. 5: Total Sensitivity Indices for Collision Probability by Orbital Altitude

3.2 Discussion

The global sensitivity values in Tables 4 through 5 highlight a few key physical phenomena. First, looking at the total global sensitivities (S_i^T), the ranking of the input variables aligns with what one might naively estimate - namely that altitude greatly impacts the estimated collision probability since altitude affects both total passive decay time as well as the distribution of objects that the satellite will pass through, the two key components to the collision probability modeling. $\frac{A}{M}$ and deorbit start year both have the next highest contributions as expected due to their direct influences

Table 5: Global Second Order Sensitivities

Sensitivity	Value (%)
$S_{y,a}$	19.70%
$S_{y,i}$	0.187%
$S_{y,m}$	1.513%
$S_{a,i}$	7.925%
$S_{a,m}$	6.195%
$S_{i,m}$	0.468%

Table 6: Global First Order and Total Sensitivities for Deorbit Time

Variable	$S_j(\%)$	S_j^T
x_y	1.769	0.0668
x_a	55.021%	0.8799
x_e	0.015	0.0021
x_i	0.004	0.0005
x_m	10.126%	0.3974

on the drag equation (Equation 2) - deorbit start year affects ρ and $\frac{A}{M}$ impacts the cross-sectional area. One particularly interesting takeaway is the importance of the deorbit start year. The global sensitivity index for S_y^T is only about half of that for semi-major axis, a much smaller gap than one might suspect intuitively. This is likely also capturing the projected debris population computed by ORDEM at the desired time, since ORDEM attempts to project future debris populations by assuming a repeat of the previous 8-year launch cycle.

However, these total sensitivity values cannot be boiled down to just the first-order sensitivities associated with each variable. While the first-order sensitivity for semi-major axis is high, for the other variables the majority of the contribution comes from secondary sensitivities which represent complex dependencies on multiple variables. One such value of note is $S_{a,i}$ which makes up $\approx 96\%$ of the total sensitivity contribution of inclination. This seems to capture the complex debris density function showed in Fig. 1. However, it is interesting to note how this distribution is less important than variables tied more to deorbit time, such as $S_{y,a}$, which is the highest valued second-order sensitivity. This can be interpreted as indicating that in the current debris environment, how long a satellite stays in orbit is much more important than exactly where it is when it begins passive decay when determining the collision risk posed to a mission.

Another result worth exploring is the binned sensitivities. For every altitude bin, the most important contributing variable by far was the deorbit start year followed by the semimajor axis. This discrepancy from the global results on semimajor axis can be attributed to the smaller altitude bins reducing the semimajor axis-based variance within each group, which in turn added more to the variance contributions of the other variables. In other words, when the semimajor axes of each point is roughly similar, other variables serve as the primary differentiator.

These binned sensitivities present a valuable insight for spacecraft designers. If a designer is attempting to lower the collision probability for a mission below 500 km, the most efficient levers would be the deorbit start year followed by the altitude. If the mission is above 500 km, the best would be the deorbit start year and the $\frac{A}{M}$ ratio. Inclination only becomes a useful dial to turn at higher altitudes as well.

Semi-major axis being a major contributor is easily explainable as the combination of higher altitudes yielding longer passive deorbit times as well as altitude choice affecting whether the mission will pass through highly congested regions. However, the prominence of deorbit year and the trends in $\frac{A}{M}$ ratio both warrant additional exploration.

3.3 Deorbit Start Year

The high influence of deorbit start year in both global and especially binned results is likely a result of two factors: 1) The influence of the 11-year solar cycle on passive deorbit times and 2) the launch rate projections in ORDEM. The relationship between lifetime collision probability estimates and deorbit times was explored in previous work computing sensitivity indices for Deorbit time [6], replicated here in Tables 6 and 7 as well as Figure 6. These indices include eccentricity (e) as an additional variable of interest.

In these results, the year in which an object deorbits has a meaningful but small impact when viewed across the global dataset (with the third highest total sensitivity index), but more importantly in the local bins there are regions where the deorbit start year becomes one of, if not the most important variable in determining deorbit time. This is due to the effects of the solar cycle, which affects drag over its roughly 11-year period. The impact of this deorbit time shift is visible in Figure 7 where there are some altitudes where a change in the deorbit start year by as little as one year can greatly impact results. For example, at 520 km going from 2026 to 2027 can change passive deorbit time from 3.3 to 5.9 years. Since collision probabilities are computed in DAS/ORDEM as propagations of an object's trajectory through predicted fluxes, the longer an object stays in orbit the greater the collision probability it will be predicted to experience. While these results partially show the influence of deorbit year on collision probability estimates, the

Table 7: Global Second Order Sensitivities for Deorbit Time

Sensitivity	Value (%)
$S_{y,a}$	3.380
$S_{y,e}$	0.021
$S_{y,i}$	0.019
$S_{y,m}$	0.067
$S_{a,e}$	0.004
$S_{a,i}$	0.000
$S_{a,m}$	28.022
$S_{e,i}$	0.013
$S_{e,m}$	0.027
$S_{i,m}$	0.001

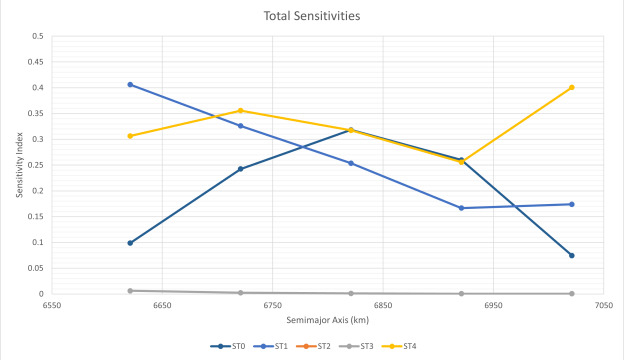

Fig. 6: Total Sensitivity Indices for Deorbit Time by Orbital Altitude

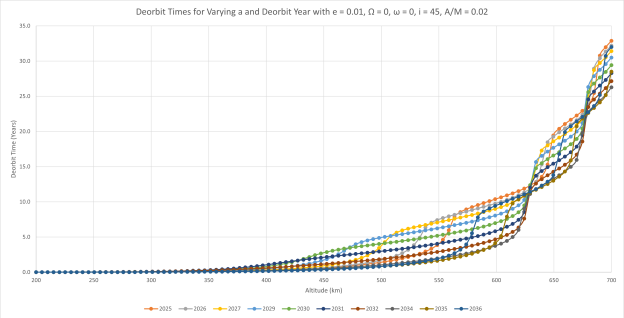

Fig. 7: Altitude and Deorbit Year vs Passive Deorbit Time

dominance of deorbit year is much higher on collision probability than it is on deorbit time, indicating there is another factor at play. $S_{y,a}$ for deorbit time is only 3.38% whereas for collision probability it is a much larger 19.70% . A likely candidate is the launch forecasting model used by ORDEM. ORDEM repeats 8-year windows of historical launch rates and assumes a 90% post-mission disposal success rate for rocket bodies and spacecraft. However, over the last 8 years launch rates have increased greatly as visible in Fig. 8 from the European Space Agency's 2024 Space Environment Report [12]. This means that the orbital population growth decreases at regular intervals. If this decrease is enough to allow the modeled disposals to decrease the total orbital population in LEO, it would explain the high sensitivity to deorbit year. Not only would the choice of deorbit year affect the mission's deorbit time via the solar cycle, but it would also potentially affect the total number of objects contributing to the flux encountered by the mission.

3.4 $\frac{A}{M}$ Dependence

Another variable worth a closer look is the $\frac{A}{M}$ ratio. Since the simulations were run with a fixed mass, this is functionally equivalent to a representation of the cross-sectional area of the satellite. This can impact collision probability

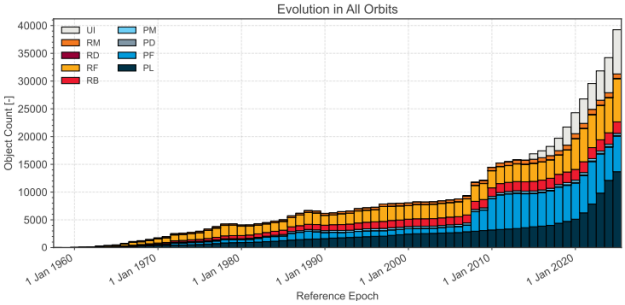

Fig. 8: ESA Space Environment Report 2024 Space Object Estimates

in two ways. First, a larger $\frac{A}{M}$ can greatly impact passive deorbit time. As seen in Table 6 and Fig. 6 the $\frac{A}{M}$ ratio is one of the largest contributors to passive deorbit time. Figure 9 shows the deorbit time as a function of semimajor axis for 3 different $\frac{A}{M}$ ratios. Particularly at higher altitudes, a change in $\frac{A}{M}$ can increase passive deorbit time by an order of magnitude, which in turn increases computed collision probability. Given this large impact, one would expect

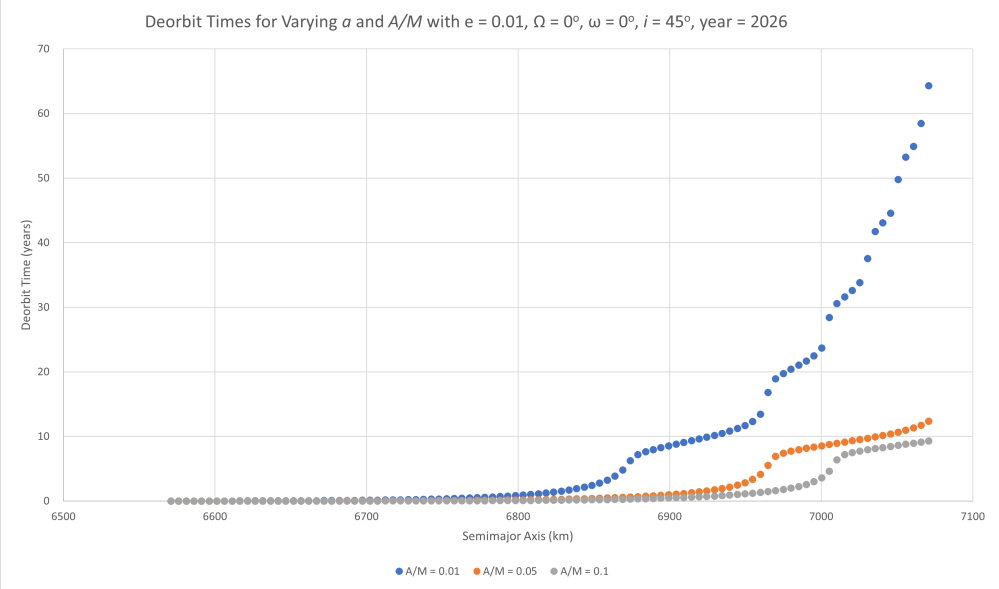

Fig. 9: Deorbit Times vs Altitude and $\frac{A}{M}$

$\frac{A}{M}$ to have a more prominent impact on collision probability, but this large effect is countered at low altitudes by the increased collision cross-sectional area implied by a higher $\frac{A}{M}$ ratio. However, at higher altitudes the increased risk from the cross-sectional area increase is outweighed by the larger changes to passive deorbit time. Figure 10 shows the evolution of collision probability as a function of $\frac{A}{M}$ ratio and altitude. Supports this theory, with the rate of change of collision probability with respect to $\frac{A}{M}$ being near 0 at the lower altitudes and increasing at the higher altitudes.

4. CONCLUSIONS

This study represents the first sensitivity analysis of NASA DAS/ORDEM estimates of lifetime collision probability that quantifies the effects of user input variations. The computed Sobol Sensitivity Indices verified prior predictions, such as the importance of altitude on the probability of collision, and highlighted deorbit year and semimajor axis as the most important input variables with the greatest impact on collision probability. They also captured the impact of known physical relationships such as the distribution of on-orbit objects by altitude/inclination and the 11-year solar cycle. Notably these indices were able to shed light on less obvious insights. The data shows that collision

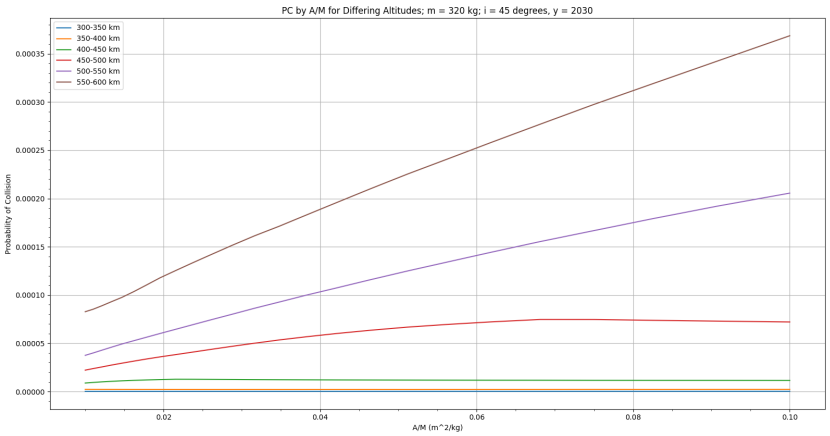

Fig. 10: PC vs Altitude and $\frac{A}{M}$

probability is actually much more dependent on deorbit year, especially when looking at variations within a smaller altitude bin. This is most likely due to a combination of solar cycle effects adjusting passive deorbit lifetime and launch rate projections within ORDEM causing fluctuations in orbital population estimates. The data also shows that for a satellite designer designing a mission below 500 km, it is minimally effective to adjust the area-to-mass ratio since the increased orbital lifetime is not sufficient to counteract the greater risk from a larger collision area. However, above 500 km the deorbit lifetime improvements become large enough to make it a useful dial to decrease collision probability. These examples highlight the value of analyzing these sensitivity indices and the opportunity they provide to gain insight on complex models of space safety metrics.

Future work to refine these indices could examine the impact of more complex variables like passive deorbit time, disambiguate factors like mass and area, and examine other metrics and models in order to uncover additional non-intuitive relationships. Additionally, while the qualitative stack ranking afforded by sensitivity indices can be useful for trade studies, a quantitative approach like a surrogate model or a regression could prove useful for more directly estimating the trade-offs between factors, as was done for passive deorbit time in previous work.

One important item of note is the implications this study has on the role of models in regulatory filings and assessing compliance. When a spacecraft operator demonstrates compliance with space safety conditions using DAS at the time of filing, the operator is not able to predict new constraints and solar weather conditions that will change the mission profile or even the physical parameters of the spacecraft. It is common for operators to slightly adjust their nominal operational orbits, redesign spacecraft components to meet mission constraints, or push their launch date due to manufacturing delays or launch provider requests, all of which can cause the actual on-orbit parameters to differ from those at the time of filing. If these discrepancies are in variables that the output is highly sensitive to for the given mission, then it is possible for the actual space safety behavior to differ from what was filed. This also highlights the importance of active deorbit plans and satellite maneuverability when it is feasible for a mission. Using on-board propulsion to rapidly deorbit and conduct collision avoidance maneuvers removes the need to rely on these variable estimates of lifetime collision probability in order to ensure compliance with regulatory requirements.

Overall, this study presents a scalable approach to quantifying the sensitivity of outputs from space safety compliance models such as DAS. The resultant sensitivity values not only provide insight into non-trivial and non-intuitive relationships between variables, but also can serve as guidelines for spacecraft operators and designers seeking to incorporate space safety concerns and regulatory compliance into their trade studies. The sensitivities highlighted by this study also bring to light potential shortcomings when using predictive metrics as a tool for ensuring safe space operations, since even minor deviations in the spacecraft parameters between time of filing and launch could have a large impact on the spacecraft's compliance.

5. REFERENCES

[1] Maarten Arnst, Christian Soize, and Kevin Bulthuis. Computation of sobol indices in global sensitivity analysis from small data sets by probabilistic learning on manifolds. *HAL Open Science*, 2021.

[2] E. Borgonovo. A new uncertainty importance measure. *Reliability Engineering and System Safety*, 2007.

[3] Dan Gabriel Cacuci. *Sensitivity and Uncertainty Analysis: Theory*. Chapman & Hall, vol. 1 edition, 2003.

[4] J.E Campbell, G.R. Carmichael, T Chai, and et al. Photosynthetic control of atmospheric carbonyl sulfide during thegrowing season. *Science*, 2008.

[5] F. Campolongo, S. Tarantola, and A. Saltelli. Tackling quantitatively large dimensionality problems. *Computer Physics Communications*, 1999.

[6] Yash Chandramouli and Liberty Shockley. Analyzing das space safety computation sensitivity to satellite design parameter variations. *IAA Space Traffic Management Conference 2025*, 2025.

[7] Lamberto Dell'Elce and Gaetan Kerschen. Probabilistic assessment of lifetime of low-earth-orbit spacecraft: Uncertainty propagation and sensitivity analysis. *Journal of Guidance, Control, and Dynamics. Vol. 38 No. 5*, 2015.

[8] J.C. Dolado-Perez, Bruno Revelin, and Romain Di-Constanzo. Sensitivity analysis of the long-term evolution of the space debris population in leo. *Journal of Space Safety Engineering, Volume 2, Issue 1*, 2015.

[9] R.L. Kelley. Using the design for demise philosophy to reduce casualty risk due to reentering spacecraft. 63rd International Astronautical Congress, 2012.

[10] Max D. Morris. Factorial sampling plans for preliminary computational experiments. *Technometrics, Vol. 33, No. 2*, 1991.

[11] James M. Murphy, David M. H. Sexton, David N. Barnett, Gareth S. Jones, Mark J. Webb, Matthew Collins, and David A. Stainforth. Quantification of modelling uncertainties in a large ensemble of climate change simulations. *Nature 430*, 2004.

[12] ESA Space Debris Office. Space environment report 2024. *European Space Agency*, 2024.

[13] ESA Space Debris Office. *Space Vehicle Dynamics and Control*. European Space Agency, 8 edition, 2024.

[14] Orbital Debris Program Office. *Debris Assessment Software User's Guide*. National Aeronautics and Space Administration, 2021. NASA/TP-20210025946.

[15] A. Saltelli. Making best use of model evaluations to compute sensitivity indices. *Computer Physics Communications*, 2007.

[16] A Saltelli, S. Tarantola, and K.P.S. Chan. A quantitative model-independent method for global sensitivity analysis of model output. *Technometrics, 41*, 1999.

[17] Andrea Saltelli, Marco Ratto, Terry Andres, Francesca Campolongo, Jessica Cariboni, Debora Gatelli, Michaela Saisana, and Stefano Tarantola. *Global Sensitivity Analysis*. John Wiley & Sons, 2008.

[18] I.M. Sobol. Global sensitivity indices for nonlinear mathematical models and their monte carlo estimates. *Math Comput Simulat*, 2001.

[19] Andrew Vavrin, Alyssa Manis, John Seago, Drake Gates, Phillip Anz-Meador, Mark Matney, and J-C Liou. Nasa orbital debris engineering model ordem 3.2 – software user guide. https://ntrs.nasa.gov/citations/20230014989, 2023. 2023-10-17.